Article | Received 16 January 2026; Revised 4 March 2026; Accepted 12 March 2026; Published 8 April 2026
https://doi.org/10.55092/neuroelectronics20260006

Supplementary data

Lossy compression with feature reduction preserves motor decoding for brain-computer interfaces

Byeongchan Jeong[1], Anh Tuan Nguyen[2], Tong Wu[3], Brian Z. H. Lim[1] and Zhi Yang[1,2,*]

[1] Department of Biomedical Engineering, University of Minnesota, Minneapolis, USA
[2] Fasikl Incorporated, Bloomington, USA
[3] IQVIA Holdings, Inc., Wayne, USA

* Correspondence author; E-mail: yang5029@umn.edu.

Table S1 presents the feature sets used for feature extraction in the main manuscript, as well as the types of features remaining after feature reduction for each dataset and transform method. The numbers in parentheses indicate the number of retained features. Feature sets that were commonly retained across transform methods are also summarized for each dataset and for the combined datasets. The corresponding decoding accuracies are reported in Table S2. Table S2 compares the decoding accuracies obtained using the retained feature sets listed in Table S1 with those reported in Table 3 of the main manuscript. For this analysis, the values in Table S2 were evaluated at the threshold scales selected after applying the Euclidean distance metric used in Figure 9 and Table 3. Finally, Figure S1 and Figure S2 present the confusion matrices for the decoding accuracies reported in Figure 9 and Table 3, respectively.

Supplementary tables

Table S1. Reduced feature identities at the balanced operating points and common reduced feature sets. Reduced features were selected using the feature-wise NRMSE criterion ($\tau_{NRMSE} = 0.5$; Methods 2.3.3) at the balanced operating points reported in Figure 9 and Table 3. Counts in parentheses denote the number of retained features; "Common" denotes the intersection across methods within each dataset, and "Dataset 1 ∩ Dataset 2" denotes the intersection shared across both datasets.

Dataset/Condition		Sym4 DWT	Haar DWT	DCT	WHT
Reduced feature sets (per method)	**Entire (14 features)**	ZC, SSC, WL, WA, MAB, MSQ, RMS, V3, LD, DABS, MFL, MPR, MAVS, WMA (14)			
	Dataset 1 Reduced	WA, MAB, RMS, V3, LD, DABS, MFL, MPR, MAVS, WMA (10)	MAB, RMS, V3, LD, DABS, MFL, MPR, MAVS, WMA (9)	ZC, WA, MAB, RMS, V3, LD, DABS, MFL, MPR, MAVS, WMA (11)	WL, MAB, RMS, V3, LD, DABS, MPR, MAVS, WMA (9)
	Dataset 2 Reduced	SSC, WL, MAB, MSQ, RMS, V3, DABS, MFL, MPR, MAVS, WMA (11)	WL, MAB, MSQ, RMS, V3, LD, DABS, MFL, MPR, MAVS, WMA (11)	SSC, WL, WA, MAB, MSQ, RMS, V3, DABS, MFL, MPR, MAVS, WMA (12)	ZC, SSC, WL, WA, MAB, MSQ, RMS, V3, DABS, MFL, MPR, MAVS, WMA (13)
Common reduced feature sets (across methods)	**Dataset 1**	MAB, RMS, V3, LD, DABS, MPR, MAVS, WMA (8)			
	Dataset 2	WL, MAB, MSQ, RMS, V3, DABS, MFL, MPR, MAVS, WMA (10)			
	Dataset 1 ∩ Dataset 2	MAB, RMS, V3, DABS, MPR, MAVS, WMA (7)			

Abbreviations: ZC, zero crossings; SSC, slope sign changes; WL, waveform length; WA, Wilson amplitude; MAB, mean absolute; MSQ, mean square; RMS, root mean square; V3, V-order 3; LD, log detector; DABS, difference absolute standard deviation; MFL, maximum fractal length; MPR, myopulse percentage rate; MAVS, mean absolute value slope; WMA, Weighted mean absolute. Feature definitions and computations follow [1].

Table S2. Decoding accuracies under enforced common reduced feature sets. Accuracies are reported at the balanced operating points (Figure 9 and Table 3) while applying the common reduced feature sets defined in Table S1.

Dataset/Condition		Sym4			Haar			DCT			WHT		
		Acc	**ΔEnt[3]**	**ΔRed[4]**	**Acc**	**ΔEnt**	**ΔRed**	**Acc**	**ΔEnt**	**ΔRed**	**Acc**	**ΔEnt**	**ΔRed**
D1[1]	**D1 Common**	89.80 ±3.73	+1.89	+0.46	89.30 ±3.69	−4.69	+1.17	87.72 ±8.51	−1.51	−2.22	88.05 ±2.67	+10.99	+7.02
	D1∩D2 Common	89.80 ±2.77	+1.89	+0.46	90.51 ±3.20	−3.48	+2.38	88.50 ±3.99	−0.73	−1.44	89.95 ±3.40	+12.89	+8.92
D2[2]	**D2 Com.**	94.38 ±1.00	+0.31	+0.10	94.34 ±0.93	+0.37	−0.14	94.66 ±0.85	+0.32	+0.29	94.25 ±0.57	+0.33	+0.07
	D1∩D2 Com.	93.93 ±0.88	−0.14	+0.35	93.42 ±1.19	−0.55	−1.06	94.49 ±0.30	+0.25	+0.22	93.61 ±0.76	−0.31	−0.57

D1[1]/D2[2] denote Dataset 1 (invasive) and Dataset 2 (non-invasive).
D1 Common and D2 Common apply the within-dataset common reduced feature sets across methods (Table S1).
D1∩D2 Common applies their cross-dataset intersection (Table S1).
ΔEnt[3]/ΔRed[4] denotes the change relative to the corresponding method's entire and reduced-feature accuracy.

Notably, in Dataset 1, WHT exhibited a larger improvement under common-set enforcement compared to other methods. This may indicate that WHT benefits more from excluding a subset of features that are particularly sensitive to reconstruction distortions.

Supplementary figures

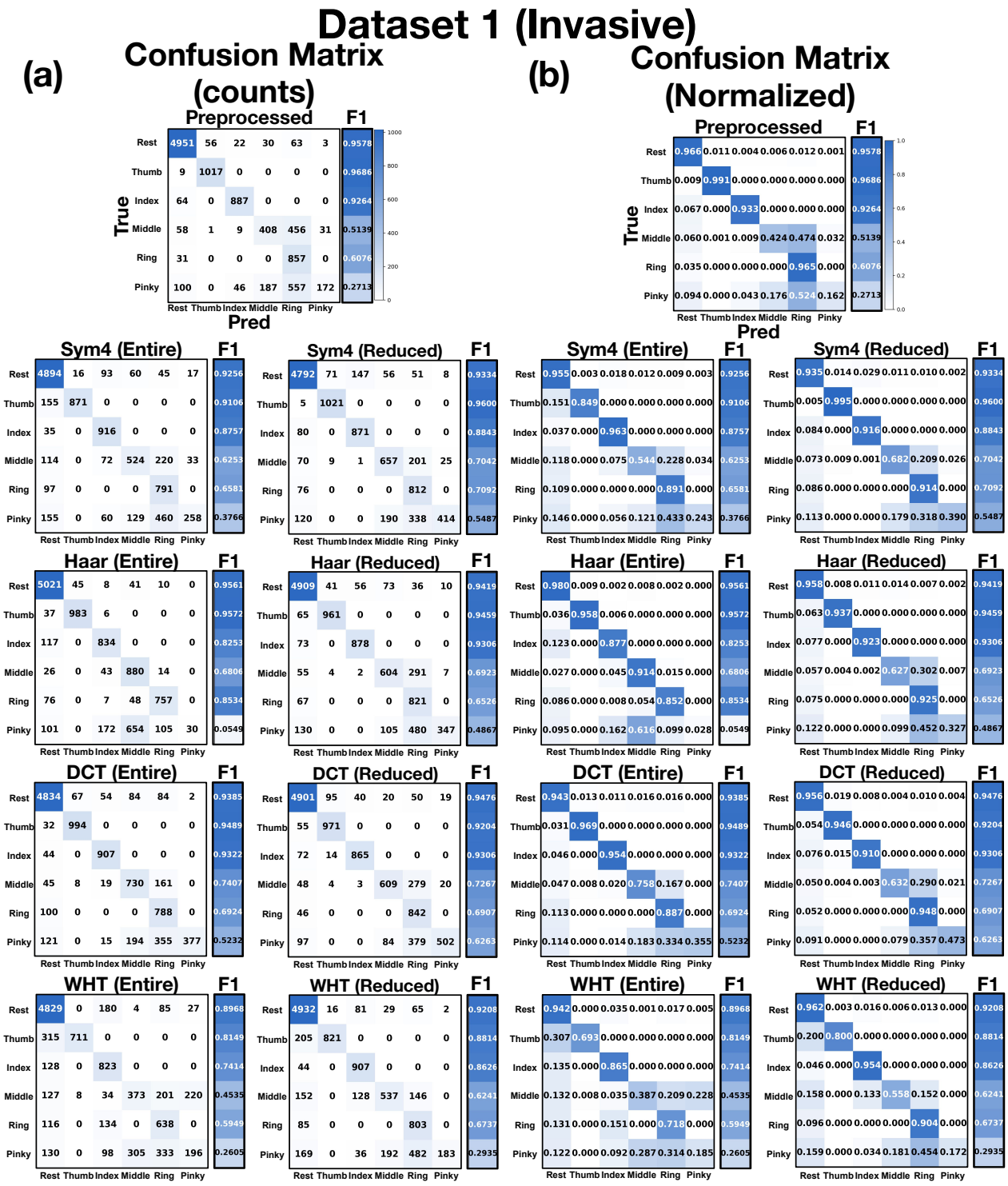

Figure S1. Confusion matrices and per-class F1 scores for Dataset 1 (invasive) at the balanced operating points. **(a)** Confusion matrices (counts) with per-class F1 scores for the preprocessed baseline and for each transform method, shown for both the Entire (14 features) and Reduced feature conditions; **(b)** The corresponding normalized confusion matrices. Balanced operating points follow the selection reported in Figure 9 and Table 3.

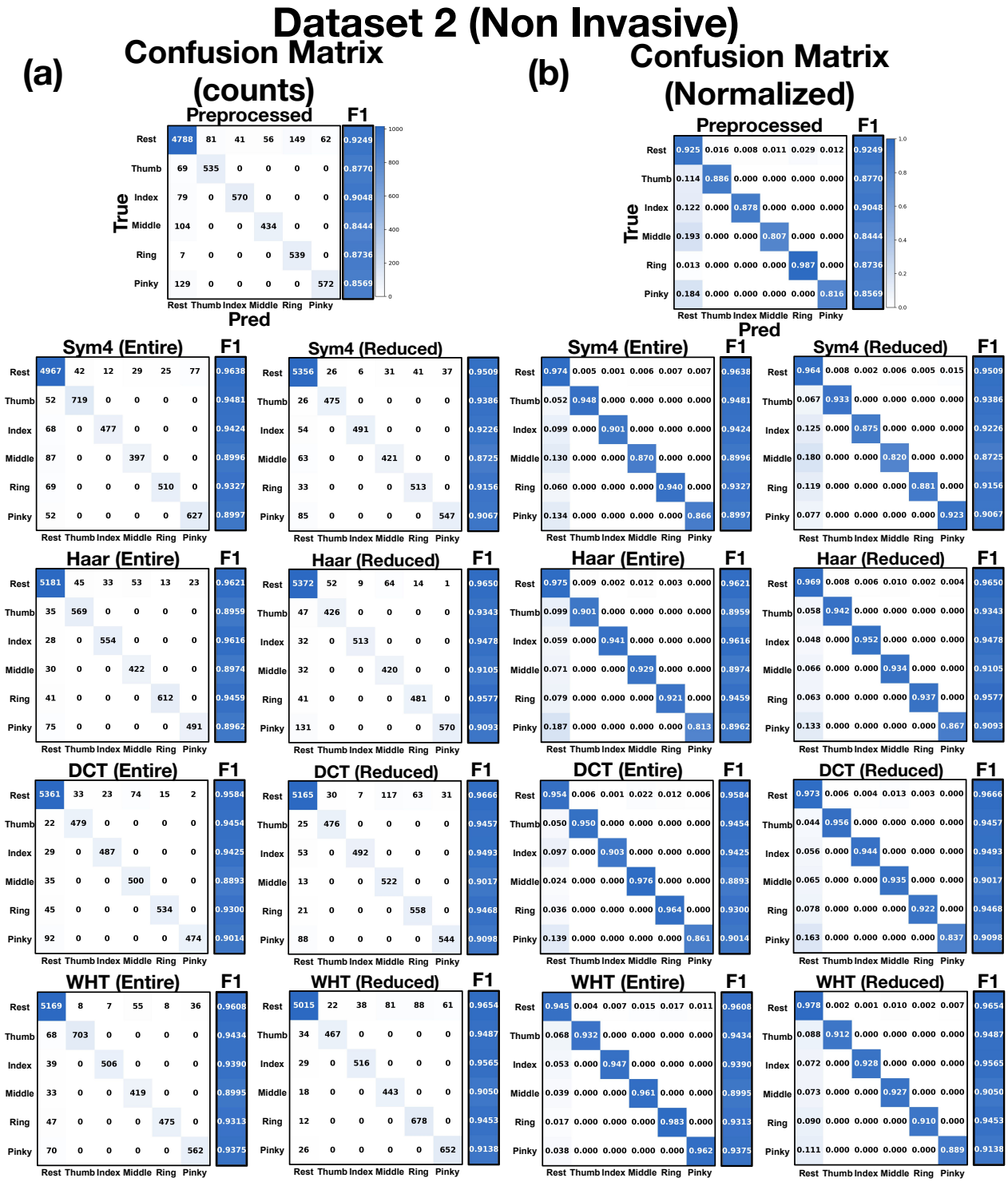

Figure S2. Confusion matrices and per-class F1 scores for Dataset 2 (non-invasive) at the balanced operating points. **(a)** Confusion matrices (counts) with per-class F1 scores for the preprocessed baseline and for each transform method, shown for both the Entire (14 features) and Reduced feature conditions; **(b)** The corresponding normalized confusion matrices. Balanced operating points follow the selection reported in Figure 9 and Table 3.

References

[1] Luu DK, Nguyen AT, Jiang M, Xu J, Drealan MW, *et al.* Deep learning-based approaches for decoding motor intent from peripheral nerve signals. *Front. Neurosci.* 2021, 15:667907.